Aggregated morphodynamic modelling of tidal inlets and estuaries

Zheng Bing Wang[1,2,4], Ian Townend[1,3], Marcel Stive[1,2]

1 College of Harbor, Coastal and Offshore Engineering, Hohai University, Nanjing, China
2 Department of Hydraulic Engineering, Faculty of Civil Engineering and Geosciences, Delft University of Technology, Delft 2600GA, the Netherlands
3 School of Ocean and Earth Sciences, University of Southampton, Southampton, UK
4 Deltares, Delft, the Netherlands

Abstract

Aggregation is used to represent the real world in a model at an appropriate level of abstraction. We use the convection-diffusion equation, as used in many coastal and estuarine morphological models, to examine the implications of aggregation as one progresses from a 3D spatial description, to a model that represents the system as a single box which exchanges sediment with the adjacent environment. We highlight how all models depend on some form of parametric closure, which needs to be chosen to suit the scale of aggregation adopted in the model. All such models are therefore both aggregated and making use of some empirical relationship to represent sub-model scale processes – it is just a matter of scale. One such appropriately aggregated model is examined in more detail (ASMITA - Aggregated Scale Morphological Interaction between Tidal basin and Adjacent coast) and used to illustrate the insight that this level of aggregation can bring to a problem by considering how tidal inlets and estuaries are impacted by sea level rise.

Key words: Tidal inlet, morphology, modelling, time and space scales, sea level rise

1. Introduction

Morphodynamic modelling of coast and estuary systems has developed rapidly over the past 30 years, with many well-established modelling tools (e.g. Delft3d, FVCOM, ASMITA), accompanied by guidance on the application of such models (e.g. Roelvink and Reniers, 2012, www.estuary-guide.net). Within this discipline, most research has focussed on the development of numerical models that solve the flow and sediment transport equations to predict the change in morphology over estuary space scales and timescales of years to decades (e.g. Dam et al., 2016; van der Wegen et al., 2009). These can be used to examine the evolution of tidal creeks, intertidal flats and channels at the local scale, where the spatial resolution is of the order of 10's of metres and the temporal resolution is seconds to hours. For morphological modelling this is usually taken to be the micro-scale (Cowell et al., 2003, who propose a scale classification of micro, O[s-yr, m-km]; meso, O[1-10^3yr, 1-10^6m]; macro, O[millennia, >10^6m]). The models used at this (micro) scale are typically governed by 'fast' hydraulic flow simulations, which adopt some form of empirical relationship to deal with sub-scale processes, such as turbulence and bed friction.

However, this is just one level of abstraction. Another well-established class of models is concerned with the larger meso-scale, where the focus is on the state of morphological features, or the morphological system. This can be both qualitative, describing the state and system behaviour, or quantitative, providing predictions at the feature/system scale. For the latter, the resolution of space and time is usually of the order of kilometres and decades to centuries, respectively.

So-called regime theory is an example of analysis at the meso-scale. This has been extensively applied in rivers, estuaries and deltas to describe key dimensions (e.g. width, depth, cross-sectional area, ebb-tidal delta volume) based on the hydraulics and in particular the characteristic discharge of the river or tidal channel (Lacey, 1930; Spearman, 2007). In the 1950s and '60s energy and entropy arguments were proposed as a theoretical basis to define the coefficients used in the earlier empirical hydraulic regime relationships, although this remains an area of some controversy (Langbein, 1963; Leopold and Langbein, 1962). Most recently, methods based on equilibrium sediment transport conditions have been used to define a system state (or regime) that is in equilibrium (Di Silvio, 1989; Stive and Wang, 2003). Although

these solve process equations that are similar to those used for micro scale models, as described above, the integration is over larger (meso) space and time scales and they have been variously referred to in the literature as aggregated, box and semi-empirical models. However, the last of these is misleading because models across all scales use some form of empirical closure to solve the governing equations. The closure of the governing equations is generally on the appropriate level of the process formulation, e.g. for small scale models on the level of the friction and/or the turbulence, for meso-scale models on the level of the aggregated sediment transport, for large-scale models on the level of the morphological elements, e.g. the entire ebb-tidal delta of a tidal inlet.

For morphological modelling, the meso-scale class of models has proved particularly useful when examining long-term change related to engineering and coastal management problems. However, there remains a lack of clarity of how this type of model relates to models used at the micro-scale. To address this, we provide a detailed account of the progressive stages of aggregation used to move from a 3D spatial description to an aggregated "box" model description. We then use the resulting mathematical description to illustrate the insights that aggregation at the macro-scale can offer. Whilst these could probably also be developed at the micro-scale, this would require huge numbers of simulations and would still lack the clarity offered by the relatively simple expressions developed by way of an aggregation at the appropriate scale – the scale of interest.

2. Stages of aggregation (from micro to meso)

To make clear the link between micro-scale and meso-scale models we make use of the convection-diffusion equation, as used in many coastal and estuarine morphological models, to examine the implications of aggregation as one progresses from a 3D spatial description (which itself involves aggregation in the closure terms) to a model that represents the system as a single box that exchanges sediment with the outside environment.

2.1. 3D to 2D aggregation (micro-scale)

We start with the 3D convection-diffusion equation governing the sediment concentration:

$$\frac{\partial c}{\partial t}+\frac{\partial uc}{\partial x}+\frac{\partial vc}{\partial y}+\frac{\partial wc}{\partial z}-\frac{\partial}{\partial x}\left(\varepsilon_x\frac{\partial c}{\partial x}\right)-\frac{\partial}{\partial y}\left(\varepsilon_y\frac{\partial c}{\partial y}\right)=w_s\frac{\partial c}{\partial z}+\frac{\partial}{\partial z}\left(\varepsilon_z\frac{\partial c}{\partial z}\right) \tag{1}$$

Herein c is sediment concentration; t is time; u, v and w are flow velocity components in the x-, y- and z-direction; ε_x, ε_y, ε_z are turbulent diffusion coefficients in x-, y- and z-direction; w_s is settling velocity. This is in fact the mass-conservation equation for sediment forming the kinetic part of the theory for suspended sediment transport. The dynamic part of the theory for suspended sediment transport is in the bed-boundary condition. At the boundary near the bed the sediment concentration, or the sediment concentration gradient, can be prescribed. Their values need to be calculated using a sediment transport formula (in the case of sand) or a formulation for the erosion rate (in the case of mud).

Equation (1) can be integrated in the vertical direction to obtain the depth-averaged advection-diffusion equation:

$$\frac{\partial h\overline{c}}{\partial t}+\frac{\partial \alpha_x\overline{u}h\overline{c}}{\partial x}+\frac{\partial \alpha_y\overline{v}h\overline{c}}{\partial y}-\frac{\partial}{\partial x}\left(D_x h\frac{\partial \overline{c}}{\partial x}\right)-\frac{\partial}{\partial y}\left(D_y h\frac{\partial \overline{c}}{\partial y}\right)=f_b \tag{2}$$

With the over-bar representing depth-averaging of the corresponding variable, and h is water depth; α_x and α_y are coefficients counting for the effects of the shapes of the vertical distribution of flow velocity and sediment concentration; D_x and D_y are dispersion coefficients; f_b is sediment exchange flux between the bed and the water column.

This can be considered as the first level of aggregation used by many micro-scale models. Note that the diffusion coefficients in the horizontal direction become dispersion coefficients as they also represent

the mixing due to the non-uniform vertical distributions of flow velocity and sediment concentration.

2.2. 2D to 1D aggregation (micro-scale)

The next level of aggregation can be carried out by integrating equation (2) over the width of a river, estuary or channel:

$$\frac{\partial A\bar{c}}{\partial t}+\frac{\partial \alpha\bar{u}A\bar{c}}{\partial x}-\frac{\partial}{\partial x}\left(AD_x\frac{\partial \bar{c}}{\partial x}\right)=F_b \tag{3}$$

With the over-bar now representing averaging over the cross-section, and A is cross-sectional area; α is coefficient counting for the effects of the distribution of flow velocity and sediment concentration within the cross-section; F_b is sediment exchange flux between the bed and the water column, f_b integrated over the width. This is the equation for suspended sediment concentration used in 1D-network models.

Equation (3) can also be written as

$$\frac{\partial h\bar{c}}{\partial t}+\frac{\partial s_x}{\partial x}+\frac{\partial s_y}{\partial y}=f_b \tag{4}$$

In which s_x and s_y represent the suspended sediment transport rate in x- and y-direction. This equation can further be aggregated by integrating over a part, or the whole, of the estuary (a morphological element). Using Green's theorem, the integration yields:

$$\frac{\partial VC}{\partial t}=\sum_i J_i+F_B \tag{5}$$

Herein V is volume of the water body of the area; J_i is sediment transport at open boundary i (positive=directed to the element, i.e. import); C is averaged sediment concentration in the element. This equation can also be derived by considering the mass-balance of sediment in the whole water body.

2.3. Further aggregation in space and time (meso scale)

Equations (2), (3), (4) and (5) can also be aggregated in time, e.g. over a tidal period or a much longer time. As an example, integration of Eq.(3) over a tidal period yields:

$$\frac{\partial u_r h\bar{c}}{\partial x}+\frac{\partial v_r h\bar{c}}{\partial y}-\frac{\partial}{\partial x}\left(D_x h\frac{\partial \bar{c}}{\partial x}\right)-\frac{\partial}{\partial y}\left(D_y h\frac{\partial \bar{c}}{\partial y}\right)=f_b \tag{6}$$

The first term representing the change of sediment storage in the water column is neglected as it becomes much less important on longer timescales than the term on the right-hand side representing the exchange with the bottom. All the other terms remain basically the same, but the parameters and variables now represent the tidally averaged values. The residual flow velocities (u_r, v_r) causes advection and the tidal flow now becomes the major mixing agent for the dispersion represented by the coefficients D_x and D_y, as elaborated by Wang et al. (2008).

Aggregation in time of Eq.(5) yields the equation used in an aggregated model, such as ASMITA (Stive and Wang, 2003).

$$\sum_i J_i+F_B=0 \tag{7}$$

2.4. Exchange between bottom and water column

The advection-diffusion equation describes a mass-balance for suspended sediment, no matter what level of aggregation is adopted. It does not describe any dynamics but only the kinetics of suspended sediment transport, because the equation itself does not provide the information on the flux of sediment exchange between the bottom and the water column. In its aggregated forms (Eqs.2-7) this flux is a term in the equation and can thus not be determined by solving the equation but needs to be prescribed. In fact, this

flux determines the morphological change as well and its formulation represents the dynamic part of the suspended sediment transport model.

For the 3D form (Eq.1) the dynamic part is introduced via the bed boundary condition. At the boundary near the bed the sediment concentration, the vertical gradient of the sediment concentration or a linear combination of the two can be prescribed. When prescribing the sediment concentration, it is often argued that the concentration near the bed can instantaneously adjust to the local flow condition and therefore the equilibrium value of the concentration can be prescribed. In fact, for steady uniform flow the solution for the vertical sediment concentration, far away from the boundary, is the equilibrium concentration profile. The prescribed value at the bed boundary is therefore by definition the equilibrium concentration. A similar argument can be made for the prescribed concentration gradient at the bed. Physically, by prescribing the concentration, the vertical flux due to settling is given but the vertical flux due to turbulent mixing is left undefined, and by prescribing the concentration gradient the opposite is true. For non-cohesive sediment the required equilibrium concentration, or equilibrium concentration gradient, depends on the flow conditions and the sediment properties and can be determined with one of the many sediment transport formulas (e.g. Soulsby, 1997; van Rijn, 1993). Note that the equilibrium values of concentration and its gradient are related to each other as at equilibrium the downwards settling flux and the upwards flux due to turbulent mixing balance each other. For cohesive sediment deposition and erosion rates according to the Krone-Partheniades formulation is often used for the bed boundary condition. According to this formulation deposition only occurs when bed shear stress is below a critical value τ_d and erosion only occurs if bed shear stress is above another critical value τ_e. With this formulation it is not always possible to define the instantaneous equilibrium concentration by balancing the deposition and erosion rates. For $\tau_d<\tau_e$ this leads to an equilibrium concentration equal to zero for $\tau<\tau_d$, undetermined for $\tau_d<\tau<\tau_e$ and infinitely large is $\tau>\tau_e$. However, if the hydrodynamic condition is fluctuating due to e.g. tide, a tide averaged equilibrium concentration can be defined. Recently Winterwerp et al. (2012) have argued that deposition always takes place, i.e. τ_d should be infinitely large. With this approach it is then possible to define the instantaneous equilibrium concentration for mud.

The advection-diffusion equations when aggregated in space but not in time (Eqs.2 & 3) are also used in micro-scale models. The flux f_b or F_b can be calculated with the Krone-Partheniades formulation for cohesive sediment, or with a formulation derived from an asymptotic solution of the (3D) advection-diffusion equation (Galappatti and Vreugdenhil, 1985; Wang, 1992) for non-cohesive sediment. These formulations require information concerning hydrodynamic conditions expressed in flow velocity, bed shear stress, etc. in addition to the sediment properties e.g. D_{50}:

$$f_b = F\left(\bar{u}, \tau, D_{50}, ...\right) \tag{8}$$

Due to the aggregation in time the required detailed information on hydrodynamic condition, as required by a sediment transport formula, or the Krone-Partheniades formulation, is no longer available. The sediment exchange flux between the bottom and the water column needs to be expressed in the available aggregated morphological and hydrodynamic parameters. This formulation, representing the dynamics of sediment, is dependent on the level of aggregation and is often a key difference between the various models. The formulations often have the form

$$f_b = \gamma w_s \left(c_e - c\right) \tag{9}$$

where w_s is the settling velocity, γ is a dimensionless coefficient, c is sediment concentration and c_e is the equilibrium value of c. This is similar as the formulation of Galappatti and Vreugdenhil (1985) for micro-scale models. The difference between the models is in the way c_e is calculated.

Di Silvio (1989) related the equilibrium concentration to the morphological state variable. As an example, for shoals influenced by wind waves he used

$$c_e \propto h^{-n} \tag{10}$$

in which h is the water depth and n is a power. It is noted that this relation implicitly defines the morphological equilibrium at which $c=c_e$ is equal to the sediment concentration prescribed at the open boundary of the model.

In the ESTMORF model (Wang et al., 1998) and ASMITA (Stive et al., 1998) the equilibrium concentration is dependent on the ratio between the morphological state variable and its equilibrium value. As an example, for the channels in ESTMORF the formulation is:

$$c_e = c_E \left(\frac{A_e}{A} \right)^n \tag{11}$$

Herein A is the cross-sectional area of the channel with A_e as its equilibrium value, c_E is a coefficient which can be considered as the global equilibrium concentration because when the whole system is in morphological equilibrium $c=c_e=c_E$ applies. The rationale behind this formulation is that the ratio A_e/A is an indication of the flow strength in the channel with respect to equilibrium, as A_e increases with increasing tidal prism. The formulation is thus analogous to a power law for sediment transport capacity.

3. Modelling at the meso-scale

Describing the system in terms of larger scale morphological elements has the advantage that empirical relations are available for morphological equilibrium. In contrast, the detailed micro-scale models often have difficulties in correctly reproducing, or even achieving, morphological equilibrium. However, the aggregation in the meso-scale schematisation also introduces difficulties in the description / representation of the hydrodynamic and sediment transport processes. To avoid such difficulties, the classic aggregated morphodynamic models assume exponential decays of disturbances with respect to morphological equilibrium (Eysink, 1990). The decay time scales are often empirically derived. Therefore, these models have been called empirical models. To our knowledge, Di Silvio (1989; 2010) was the first to introduce a suspended sediment transport module into an aggregated (in time) morphodynamic model. The long-term averaged sediment concentration field is simulated directly with an advection-diffusion equation, just like a micro-scale model that solves the instantaneous sediment concentration field. In addition, the local equilibrium value for the long-term averaged suspended sediment concentration is defined and related to the local morphological state variable following some physical arguments, and again this is conceptually the same as a micro-scale model. As an example, the equilibrium (long-term averaged sediment) concentration on shoals is argued to be inversely proportional to a power of the local water depth for given wind and wave climates. By relating the local equilibrium concentration to the morphological equilibrium, the aggregated morphodynamic models ESTMORF (Wang et al., 1998) and ASMITA (Spearman, 2007; Stive et al., 1998; Stive and Wang, 2003; Townend et al., 2016a) have been developed. These models have proven to be effective for modelling long-term morphological development in estuaries (e.g. Townend et al., 2007; Wang and Townend, 2012) and tidal inlet systems (Kragtwijk et al., 2004; van Goor et al., 2003). They combine the empirical relations for morphological equilibrium with process-modelling of suspended sediment transport and therefore have often been classified as hybrid or semi-empirical models.

The previous section makes it clear that the essential difference between meso-scale and micro-scale models (e.g. ASMITA and Delft3D) is the level of aggregation rather than the degree in which their formulations contain empirical elements. They both use the advection-diffusion equation for the suspended sediment transport. The formulations concerning sediment dynamics, i.e. the exchange between bed and water column, contain empirical elements in both models. ASMITA makes use of the empirical relations for morphological equilibrium and Delft3D uses a sediment transport formula which is also empirical in character. The empirical elements in both models also involve the same degree of uncertainty. In this sense,

it is not meaningful to classify the two types of models as respectively (semi-)empirical and process based. These models only differ in the level of abstraction that is used to represent the real world.

In addition to the aggregation level and the formulation for the sediment exchange flux between bed and water column, the hydrodynamic module helps to differentiate the various models. Obviously, the implemented hydrodynamic module depends to a large extent on the aggregation level of the model. As an example, the models ESTMORF (Wang et al., 1998) and ASMITA (Stive et al., 1998) are based on the same type of formulations. However, ESTMORF can be coupled to a (micro-scale) 1D network hydrodynamic model to simulate the required aggregated hydrodynamic parameters of tidal volume and tidal range, as can various other hybrid models (e.g. O'Connor et al., 1990; Wright and Townend, 2006). In contrast, due to the higher level of aggregation, ASMITA calculates the tidal prism for the prescribed tidal range and plan area. Micro-scale models can be 1D, 2D or 3D depending on the hydrodynamic module.

3.1. ASMITA formulation

ASMITA (Aggregated Scale Morphological Interaction between Tidal basin and Adjacent coast) was first proposed by Stive et al. (1998) for modelling long-term morphological development of tidal inlet systems in the Wadden Sea.

ASMITA has a high level of spatial aggregation. A tidal inlet system is schematised into a limited number of morphological elements, at a level like that of the ebb-tidal delta as described by (Walton and Adams, 1976). For each element a water volume below a certain reference level or a sediment volume above a certain reference plane (not necessarily horizontal) acts as the integral state variable. A tidal inlet is typically schematised into the following three elements (Fig.1): The ebb-tidal delta, with its state variable V_d = total excess sediment volume relative to an undisturbed coastal bed profile; The inter-tidal flat area in the tidal basin, with its state variable V_f = total sediment volume between MLW (mean low water) and MHW (mean high water); The channel area in the tidal basin, with its state variable V_c = total water volume below MLW.

Figure 1 shows that the adjacent coastal areas, which can exchange sediment with the inlet system, are considered as an open boundary, ‘the external world’. Tidal flats are depicted as a sediment volume (Figure 1(c)) but it is also possible to represent tidal flats by the volume of water over the tidal flats (Townend et al., 2016a).

Although commonly used for a tidal inlet system, this 3 elements-schematisation is not the only possible schematisation. In fact, an ASMITA model can contain any number of inter-connected morphological elements. In this context it is relevant to mention that the application of the ASMITA model to the Waddensea basins uses the fact that the flood-tidal delta extends over the whole back basin, which is not generally the case. The US east coast has many tidal basins with a flood tidal delta confined to a location near the inlet opening. This would require a different set of elements to represent the system.

Anyhow, a necessary requirement is that the morphological equilibrium of each element is defined and can be evaluated from the available (aggregated) hydrodynamic parameters in the model. In the following, this 3-element schematisation is used to explain the model formulation and to demonstrate some applications. In addition, a 1-element model is used to explain certain points, in which the whole back barrier basin of the tidal inlet is considered as a single morphological element with the state variable water volume V in the basin below MHW.

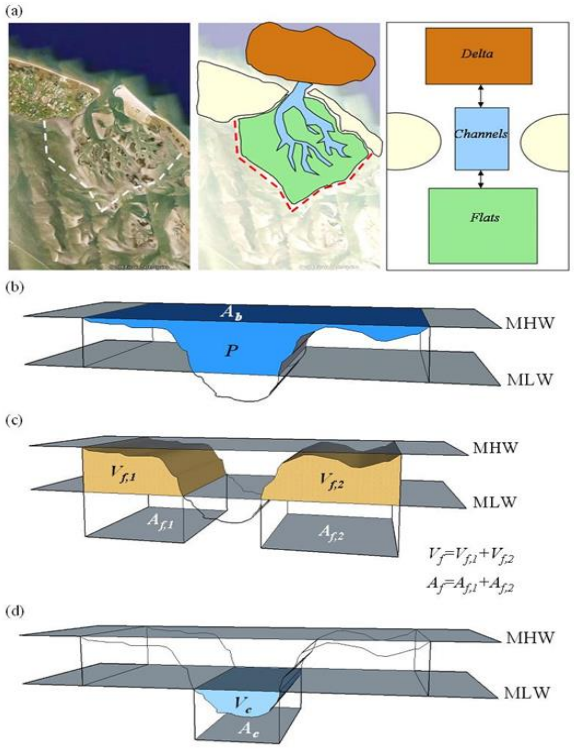

Fig.1. The 3-elements schematisation for a tidal inlet in ASMITA and the definitions of the hydrodynamic and morphological parameters tidal prism P (b), area A_f and volume V_f of tidal flats (c), area A_c and volume V_c of channels (d). After Lodder et al (2019).

The formulation of the ASMITA model has been detailed in various publications (Stive et al., 1998; van Goor et al., 2003, Kragtwijk et al., 2004, Townend et al., 2016). For completeness the basis of a 3-element model suitable for the exploration of the implications of sea level rise in tidal inlets and estuaries is provided in the Supplementary Information.

4. Impact of Sea Level Rise on Tidal Inlets

Aggregation to a particular scale allows the modeller to focus on system states, or flows in and out of the system. Choosing an appropriate scale of aggregation can make certain problems more tractable, or provide greater insight into the system dependencies. This is illustrated by considering the sensitivity of tidal inlets to sea level rise, using the formulation derived for the meso-scale. For simplicity we adopt the ASMITA formulation for a single element (combined channel and tidal flat with no delta). Previous work examined the potential for tidal inlet systems to drown (Rossington et al., 2007; van Goor et al., 2003). The analysis that follows is similar but, in more detail, to highlight how the various system parameters influence the sensitivity of the system to sea level rise.

The single element ASMITA model for a tidal basin with the water volume below high water, V, as the state variable reads:

$$\frac{dV}{dt} = \frac{w\delta c_E A_b}{\delta + wA_b}\left[\left(\frac{V_e(t)}{V(t)}\right)^n - 1\right] + A_b R \tag{12}$$

Herein V_e is equilibrium volume (equilibrium without sea-level rise, i.e. R=0) of the basin volume, V, R is sea level rise rate and A_b is the basin area. Exchanges and transport are defined in terms of a set of parameters (see SI for details), where w is the vertical rate of exchange, c_E is the global equilibrium concentration, δ is the horizontal rate of exchange and n is the transport coefficient. A dynamic equilibrium is achieved for a constant rate of sea-level rise if the volume V is constant, thus:

$$\frac{dV}{dt} = \frac{w\delta c_E A_b}{\delta + wA_b}\left[\left(\frac{V_e(t)}{V(t)}\right)^n - 1\right] + A_b R = 0 \tag{13}$$

The dynamic equilibrium is only possible if R is smaller than a critical value R_c, with:

$$R_c = \frac{w\delta c_E}{\delta + wA_b} \tag{14}$$

For the dynamic equilibrium state, we have:

$$\frac{V}{V_e} = \left(1 - \frac{R}{R_c}\right)^{\frac{-1}{n}} \tag{15}$$

This solution is depicted in Fig.2 for n=2, which also shows the solution for the linear model. The linear model is derived by linearizing Eq.(12) around V=V_e:

$$\frac{\mathrm{d}V}{\mathrm{d}t} = \frac{V_e - V}{T} + A_b R \tag{16}$$

Herein T is the morphological timescale

$$T = \frac{1}{nc_E}\left(\frac{V_e}{wA_b} + \frac{V_e}{\delta}\right) \tag{17}$$

Comparison between the equations (14) and (17) yields a relation between T and R_c.

$$R_c = \frac{V_e}{nTA_b} \quad \text{or} \quad T = \frac{V_e}{nR_c A_b} \tag{18}$$

A dynamic equilibrium for a constant rate of sea-level rise is again achieved if V no longer changes in time, thus:

$$\frac{\mathrm{d}V}{\mathrm{d}t} = \frac{V_e - V}{T} + A_b R = 0 \tag{19}$$

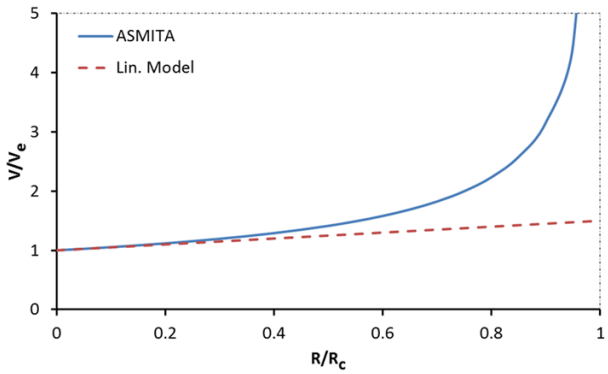

Figure 2. Relation between the dynamic equilibrium volume V (normalised by the original equilibrium volume V_e) and the sea-level rise rate R (normalised by the critical rate R_c).

This leads to

$$V = V_e + A_b RT = V_e\left(1 + \frac{R}{nR_c}\right) \tag{20}$$

4.1. Assessing the sensitivity of a system to the rate of sea level rise

Considering the system as a single element, the non-linear equation can be used to determine the sensitivity of the system to a given (constant) rate of sea level rise, as indicated by Eq.(14). The limiting rate of sea level rise is determined by four parameters and it is instructive to examine how the limiting rate varies as these parameters vary. Typical ranges for each parameter are defined in Table 1. The way in which each of these parameters influences the limiting rate of sea level rise is shown in Fig.3 (note that the

scale of the y-axis is different for each plot).

Table 1

Typical ranges for the parameters that determine the limiting rate of sea level rise for a single element

Parameter	Description	Range
w_s	Vertical exchange	1e-5 – 1e-3 ms^{-1}
δ	Horizontal exchange	500-3000 m^3s^{-1}
c_E	Equilibrium concentration	0.00002-0.0002 (-)
A_b	Surface area of basin	10^6-10^8 m^2

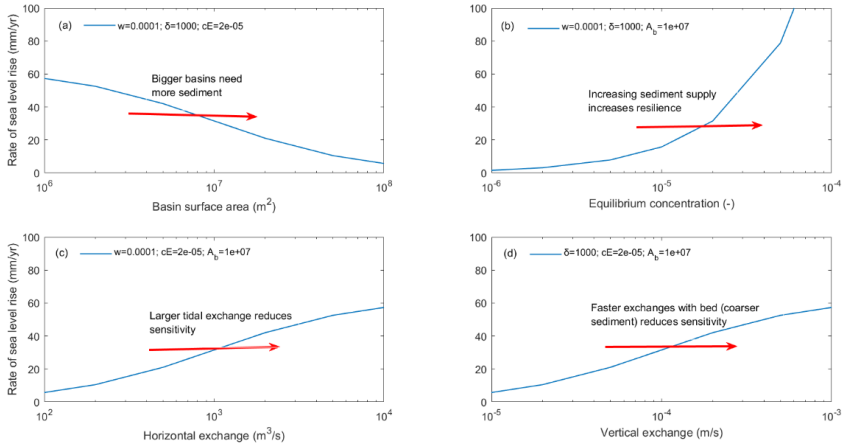

Figure 3. Plots to illustrate the limiting rate of sea level rise for (a) basin surface area, (b) equilibrium concentration, (c) horizontal exchange and (d) vertical exchange

The joint influence of the parameters is illustrated in Fig. 4. The left plot shows the combined influence of the size of the basin and the availability of sediment. The right plot shows the combined influence of the rates of horizontal and vertical exchange.

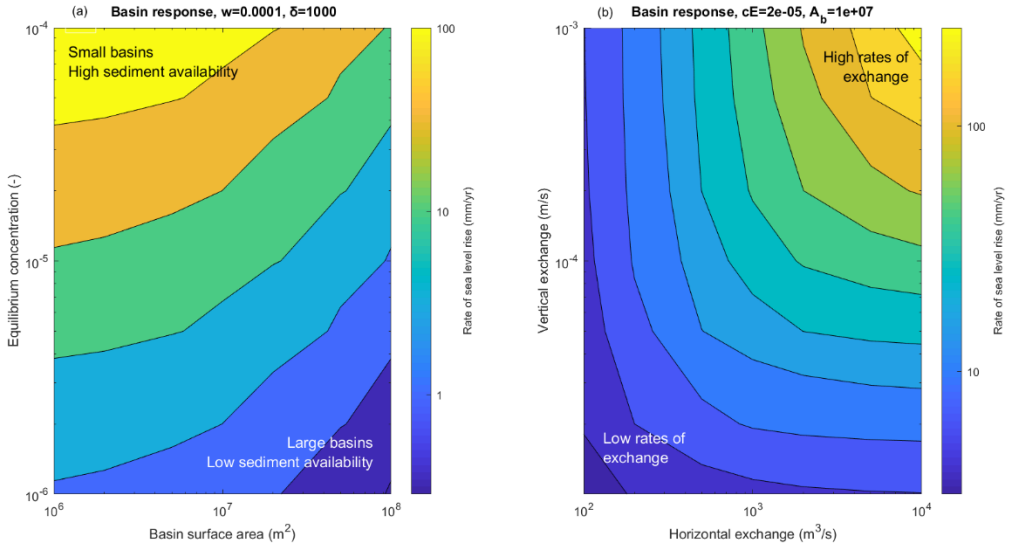

Figure 4. Limiting rate of sea level rise for (a) basin area and equilibrium concentration and (b) horizontal and vertical exchange rates

4.1.1. Relative importance of the parameters

For the range of parameters considered there is a similar degree of sensitivity to basin size, and the rates of vertical and horizontal exchange. There is a much larger variation for the range of equilibrium concentrations considered. This range represents the range from limited supply to relatively turbid systems

and highlights the importance of sediment supply. When coupled with basin size, this can have a significant effect on the system's ability to keep pace with sea level rise. Large basins with limited sediment supply are more likely to "drown" and small basins with plentiful supply should be able to maintain their form even if rates of sea level increase dramatically. In a similar manner, high rates of exchange (vertical or horizontal) increase the system resilience to rapid sea level rise.

4.1.2. Sensitivity to sea level rise

Fjords, Fjards and Rias all have limited sediment supply. Arguably Fjords and Fjards are already drowned systems. However, the potential consequence for Rias, as found in the south-west of the UK, is that they could also be progressively drowned as a result of more rapid rates of sea level rise. For coastal plain, tidal inlets and drowned valley systems, the system setting will be important. Those that have macrotidal conditions are likely to be less sensitive than those that are in locations that are micro-tidal because of the larger horizontal exchange. Similarly, sandy systems are likely to be less sensitive than muddy ones because the vertical exchange will be higher (sand has a larger settling velocity). However, in all cases, the availability of sediment will be critical. The background supply may be suspended load or bed load and may be sourced from the river or the marine environment. In this model this is represented by the equilibrium concentration; an important parameter when assessing whether the system remains healthy, or degrades; as illustrated by the changes in Venice over the last two centuries (Townend, 2010).

It is important to recognize that Eq. (38) treats the estuary system as a single element. This is, of course, a gross simplification. The ASMITA model subdivides the system into the main geomorphological elements, namely channel, tidal flat and delta. Introducing this additional sub-division results in different responses for the different types of element. In most cases the tidal flats (comprising a smaller volume and being furthest from the source of sediment) are significantly more sensitive to sea level rise than the tidal channel and delta components of the estuary. Consequently, several studies in the literature have shown that estuarine systems that include intertidal flats have the capacity to adapt to rates of sea level rise in the range of 5-30 mm/year (Rossington et al, 2007).

4.2. ASMITA applications

ASMITA is meant for simulating long-term large-scale morphological development of tidal inlet systems. It was originally developed for the tidal inlet systems in the Wadden Sea (Stive et al., 1998). The first applications to the Dutch Wadden Sea concerning the response to human interferences (Kragtwijk et al., 2004) and to sea-level rise (Van Goor et al., 2003) were summarized by Stive and Wang (2003). Later, the model has been applied to the Dutch Wadden Sea in e.g. EIA studies for gas and salt mining to other systems in the world including estuaries (Townend et al., 2007; Rossington et al., 2011). It has also been implemented as a module in the DIVA model for evaluating the impact of climate change on the worldwide coastal system (Hinkel, 2013). We refer to Townend et al. (2016a; Townend et al., 2016b) for more discussions on ASMITA and its applications. Here we discuss an application of the model to evaluate the impact of relative sea-level rise in the Wadden Sea tidal inlet systems.

The Dutch Wadden Sea consists of a series of tidal inlets with their tidal basins (Fig.5). Multiple large and small-scale human interventions in the past have basically fixed the boundaries of the Wadden Sea. The two recent major interventions are the closures of the Zuiderzee (1932) and the Lauwerszee (1969), and they are still influencing the morphological development (Elias et al., 2012; Wang et al., 2018; Wang et al., 2012). Due to the closure of the Zuiderzee the western part of the Dutch Wadden Sea (Texel, Eierlandse Gat and Vlie Inlets) is still far from morphodynamic equilibrium (Wang *et al*., 2018).

Historically, the morphological development of this system, consisting of barrier islands separated by tidal inlets and back-barrier basins with channels, tidal flats and saltmarshes, has been closely related to sea-level rise. It was formed some c. 7000 years ago under the influence of a rising sea level. The

development of basins depends on the balance between sediment accretion and the relative sea-level rise rate (Nichols, 1989). Beyond a critical rate of relative sea-level rise (where 1m/century is a ball-park number), sediment import becomes insufficient resulting in drowning of the basins (Carrasco et al., 2016; Deltacommissie, 2008; Stive et al., 1990; van der Spek and Beets, 1992; van Goor et al., 2003). The relative sea-level rise is the sea-level rise plus the sea-floor subsidence due to e.g. gas and salt extraction.

.

Fig.5. Tidal basins in the Dutch Wadden Sea

Anticipating that worldwide sea-level rise will accelerate (KNMI, 2017; Le Bars et al., 2017; Meehl, 2007) a study on the Dutch Wadden Sea has been carried out, resulting in a series of position papers coordinated by the Wadden Academy in the Netherlands. Vermeersen et al. (2018) projected three scenarios' for future sea-level rise in the Dutch Wadden Sea until 2100, following the Representative Concentration Pathways (RCP2.6, RCP4.5 and RCP8.5). Fokker et al. (2018) predicted the sea-bed subsidence due to gas and salt extraction in the coming decades. The morphological response of the Dutch Wadden Sea to the sea-level rise and subsidence (together the relative sea-level rise) was projected by Wang et al. (2018), on the basis of ASMITA model results and supported by observations concerning the morphological development since 1926. The ASMITA model used was the same as that due to Van Goor et al. (2003), with the most up-to-date parameter settings for the tidal inlet systems shown in Table 2.

Table 2
ASMITA model parameters for the tidal inlets in the Dutch Wadden Sea

Inlet	**Texel**	**Eierland**	**Vlie**	**Ameland**	**Pinkegat**	**Zoutkamp**
Basic configuration: tidal range and the horizontal areas of the three elements						
2a (m)	1.65	1.65	1.90	2.15	2.15	2.25
A_f (km^2)	133	105	328	178	38.1	65
A_c (km^2)	522	52.7	387	98.3	11.5	40
A_d (km^2)	92.53	37.8	106	74.7	34	78
Parameters influencing morphological time scale						
n (-)	2	2	2	2	2	2
C_E (-)	0.0002	0.0002	0.0002	0.0002	0.0002	0.0002
w_{sf}(m/s)	0.0001	0.0001	0.0001	0.0001	0.0001	0.0001
w_{sc}*(m/s)*	0.0001	0.00005	0.0001	0.00005	0.0001	0.0001
w_{sd}*(m/s)*	0.00001	0.00001	0.00001	0.00001	0.00001	0.00001
δ_{od} (m^3/s)	1550	1500	1770	1500	1060	1060

δ_{dc} (m^3/s)	2450	1500	2560	1500	1290	1290
δ_{cf} (m^3/s)	980	1000	1300	1000	840	840
Initial conditions: volumes of the three morphological elements in 1970						
$V_{f0}(Mm^3)$	51.5	55	162	120	29.6	69
$V_{c0}(Mm^3)$	2160	106	1230	302	18.5	177
$V_{d0}(Mm^3)$	509.1	132	369.7	131	35	151
Parameters for defining the morphological equilibrium						
V_{fe} (Mm^3)	151	57.83	190	131.2	30.3	70
α_c (10^{-6})	10	13.13	9.6	10.241	10.14	27.266
α_d (10^{-3})	4.025	8	2.662	2.92157	6.9278	9.137

Following the approach of Van Goor et al. (2003), the results were presented as probability of drowning as a function of the rate of SLR, which has been obtained by considering all the relevant model parameters as stochastic variables. Based on this probability distribution an uncertainty range for the critical rate of SLR can be given, see Table 4. In this table, the value corresponding to a probability of 16% for drowning is the median value minus the standard deviation (if the distribution is a normal one). However, the values for Texel and Vlie Inlet appear to be unrealistic, as the lower limits are lower than the observed sedimentation rates in the past. The observed sedimentation rates in these two inlets correspond to about 30% probability for drowning. Therefore, the range based on the 30% probability is also given in Table 3.

By comparing the median values in this table to the sea-level rise scenarios presented by Vermeersen et al. (2018) and the sea-bed subsidence projections by Fokker et al. (2018) Wang et al. (2018) concluded that the critical speed of relative sea-level rise will not be exceeded for the RCP2.6 scenario in any of the basins in the Dutch Wadden Sea. For the RCP4.5 scenario it will be exceeded in only the Vlie basin starting from 2030, for the RCP8.5 scenario in Texel Inlet basin starting from 2050, in the Vlie basin from 2030 and in the Ameland Inlet basin from 2100. It is noted that exceedance of the critical value does not mean that a tidal basin will drown (loss of all intertidal flats) immediately. In fact, it is concluded that none of the considered tidal basins will drown before 2100, even for the RCP8.5 scenario. However, the accelerated sea-level rise will cause loss of part of the intertidal flats. The loss will be noticeable in 2050 for the RCP8.5 scenario and in 2100 for the RCP4.5 scenario.

Table 3

Critical sea-level rise rates (mm/year) for the tidal basins in the Dutch Wadden Sea for five values of probabilities of drowning. The median value (50% probability) is used for the projections of the morphological response.

Inlet	Texel	Eierland	Vlie	Ameland	Pinkegat	Zoutkamp
16%	4.5	11.6	4.1	6.7	21.1	11.1
30%	5.5	14.2	5.0	8.2	25.8	13.5
50%	**7.0**	**18.0**	**6.3**	**10.4**	**32.7**	**17.1**
70%	8.1	20.9	7.3	12.1	37.9	19.8
84%	9.5	24.4	8.5	14.1	44.3	23.1

5. Conclusions

Aggregation is a valuable means by which a modeller can focus on representing the real world at an appropriate level of abstraction, choosing the attributes and system states of interest. Too crude an abstraction may provide simplicity but insufficient resolution of the problem, whereas inclusion of too

much detail may make the model computationally intensive, or even intractable. Hence the correct choice is important for efficiency but more importantly for the clarity of insight that can be obtained.

Using morphological models of tidal inlets and estuaries as an example, we have shown that the aggregation is a process of progressively grouping terms, or integrating over spatial and temporal scales. Thus, in the example presented the models at the different scales (micro and meso) are solving the same equations just at different levels of resolution. Importantly, the need for some form of empirical closure scheme is present at all scales. Hence the models are all empirical to some degree.

The insights to be gained from aggregation to the scale of interest have been illustrated for the case of sea level rise. With some manipulation of the governing equations at the meso-scale it is possible to show how a tidal inlet subject to sea level rise is likely to respond and how this varies as a function of system size, tidal range, sediment supply and type of sediment. Such a relatively simple examination of the key dimensions of the problem would be much harder to achieve using an equivalent micro-scale model.

Acknowledgement

This study was carried out within the framework of Coastal Genesis 2 project funded by Rijkswaterstaat, and co-founded by NWO via the SEAWAD project and the Dutch Royal Academy of Sciences via the project Coping with Deltas in Transition within the framework of Programme Scientific Strategic Alliances between China and the Netherlands.

References

Carrasco, A.R., Ferreira, Ó., Roelvink, D., 2016. Coastal lagoons and rising sea level: A review. Earth Science Reviews, 154, 356-368 [https://doi.org/10.1016/j.earscirev.2015.11.007].

Cowell, P.J., Stive, M.J.E., Niedoroda, A., de Vriend, H.J., Swift, D., Kaminsky, G.M., Capobianco, M., 2003. The coastal-tract (Part 1): A conceptual approach to aggregated modelling of low-order coastal change. Journal of Coastal Research, 19(4), 812-827.

Dam, G., van der Wegen, M., Labeur, R.J., Roelvink, D., 2016. Modeling centuries of estuarine morphodynamics in the Western Scheldt estuary. Geophysical Research Letters, [https://doi.org/10.1002/2015gl066725].

Deltacommissie, 2008. Working together with water, Report of Deltacommissie, Netherlands.

Di Silvio, G., 1989. Modelling the morphological evolution of tidal lagoons and their equilibrium configurations. IAHR Congress. IAHR, pp. C-169-C-175.

Di Silvio, G., Dall'Angelo, C., Bonaldo, D., Fasolato, G., 2010. Long-term model of planimetric and bathymetric evolution of a tidal lagoon. Continental Shelf Research, 30(8), 894-903 [https://doi.org/10.1016/j.csr.2009.09.010].

Elias, E.P.L., van der Spek, A.J.F., Wang, Z.B., de Ronde, J.G., 2012. Morphodynamic development and sediment budget of the Dutch Wadden Sea over the last century. Netherlands Journal of Geosciences, 91, 293-310 [https://doi.org/10.1017/s0016774600000457].

Eysink, W.D., 1990. Morphological response of tidal basins to change. 22nd International Conference on Coastal Engineering. ASCE, Delft, pp. 1948-1961 [https://doi.org/10.1061/9780872627765.149].

Fokker, P.A., van Leijen, F., Orlic, B., van der Marel, H., Hanssen, R., 2018. Subsidence in the Dutch Wadden Sea. Netherlands Journal of Geosciences, 97(3), 129-181 [https://doi.org/10.1017/njg.2018.9].

Galappatti, G., Vreugdenhil, C.B., 1985. A depth integrated model for suspended sediment transport. Journal of Hydraulic Research, 23(4), 359-375 [https://doi.org/10.1080/00221688509499345].

Hinkel, J., Nicholls, R.J., Tol, R.S.J., Wang, Z.B., Hamilton, J.M., Boot, G., Vafeidis, A.T., McFadden, L., Ganopolski, A. & Klein, R.J.T., , 2013. A global analysis of erosion of sandy beaches and sea-level rise: An application of DIVA. Global and Planetary Change, 111, 150-158 [https://doi.org/10.1016/j.gloplacha.2013.09.002].

KNMI, 2017. Extreme zeespiegelstijging in de 21e eeuw. Koninklijk Nederlands Meteorologisch Instituut (KNMI). .

Kragtwijk, N.G., Stive, M.J.F., Wang, Z.B., Zitman, T.J., 2004. Morphological response of tidal basins to human interventions. Coastal Engineering, 51, 207-221 [https://doi.org/10.1016/j.coastaleng.2003.12.008].

Lacey, G., 1930. Stable channels in Alluvium. Minutes of the Proceedings of the Institution of Civil Engineers, 229, 259-292, [https://doi.org/10.1680/imotp.1930.15592].

Langbein, W.B., 1963. The hydraulic geometry of a shallow estuary. Bulletin of Int Assoc Sci Hydrology, 8(3), 84-94 [https://doi.org/10.1080/02626666309493340].

Le Bars, D., Drijfhout, S., De Vries, H., 2017. A high-end sea level rise probabilistic projection including rapid Antarctic ice sheet mass loss. Environmental Research Letters, 12(4), 044013 [https://doi.org/10.1088/1748-9326/aa6512].

Leopold, L.B., Langbein, W.B., 1962. The concept of entropy in landscape evolution. Professional Paper 500-A, United States Government Printing Office, Washington [https://doi.org/10.3133/pp500a].

Lodder, Q.J., Wang, Z.B., Elias, E.P.L., van der Spek, A.J.F., de Looff, H., Townend, I.H., 2019. Future Response of the Wadden Sea Tidal Basins to Relative Sea-Level rise—An Aggregated Modelling Approach. Water, 11(10) [https://doi.org/10.3390/w11102198].

Meehl, G., Stocker, T.F., Collins, W.D., Friedlingstein, P., Gaye, A.T., Gregory, J.M., Kitoh, A., Knutti, R., Murphy, J.M., Noda, A., Raper, S.C.B., Watterson, I.G., Weaver, J. & Zhao, Z.C., 2007. Global climate projections. , 2007. Global climate projections. In: S. Solomon, Qin, D., Manning, M., Chen, Z., Marquis, M., Averyt, K.B., Tignor, M. & Mille, H.L. (Ed.), Climate Change 2007: The Physical Science Basis. Contribution of Working Group 1 to the Fourth Assessment Report of the Intergovernmental Panel on Climate Change. Cambridge University Press, Cambridge, UK, pp. 996.

O'Connor, B.A., Nicholson, J., Rayner, R., 1990. Estuary geometry as a function of tidal range. International Conference of Coastal Engineering. American Society of Civil Engineers, pp. 3050-3062 [https://doi.org/10.1061/9780872627765.233].

Roelvink, D., Reniers, A., 2012. A guide to modelling coastal morphology. Advances in Coastal and Ocean engineering, 12. World Scientific Publishing, Singapore.

Rossington, K., Nicholls, R.J., Knaapen, M.A.F., Wang, Z.B., 2007. Morphological Behaviour of UK Estuaries under Conditions of Accelerating Sea Level Rise. In: C.M. Dohmen-Janssen, S.J.M.H. Hulscher (Eds.), RCEM2007. River, Coastal and Estuarine Morphodynamics. Taylor & Francis [https://doi.org/10.1201/noe0415453639-c16].

Soulsby, R., 1997. Dynamics of marine sands. Thomas Telford, London.

Spearman, J., 2007. Hybrid Modelling of Managed Realignment. TR157, HR Wallingford, Wallingford, UK.

Stive, M.J.F., Capobianco, M., Wang, Z.B., Ruol, P., Buijsman, M.C., 1998. Morphodynamics of a tidal lagoon and adjacent coast. In: J. Dronkers, M.B.A.M. Scheffers (Eds.). Physics of Estuaries and Coastal Seas: 8th International Biennial Conference on Physics of Estuaries and Coastal Seas, 1996. A A Balkema, pp. 397-407.

Stive, M.J.F., Roelvink, J.A., de Vriend, H.J., 1990. Large-scale coastal evolution concept; The Dutch Coast, Paper No. 9. In: C.J. Louisse, M.J.F. Stive, J. Wiersma (Eds.), The Dutch Coast; Report of a session on the 22nd International Conference on Coastal Engineering 1990, pp. 13 [https://doi.org/10.1061/9780872627765.150].

Stive, M.J.F., Wang, Z.B., 2003. Morphodynamic modelling of tidal basins and coastal inlets. In: C. Lakkhan (Ed.), Advances in coastal modelling. Elsevier Sciences, Amsterdam, pp. 367-392 [https://doi.org/10.1016/s0422-9894(03)80130-7].

Townend, I.H., 2010. An exploration of equilibrium in Venice Lagoon using an idealised form model. Continental Shelf Research, 30(8), 984-999 [https://doi.org/10.1016/j.csr.2009.10.012].

Townend, I.H., Wang, Z.B., Rees, J.G., 2007. Millennial to annual volume changes in the Humber Estuary. Proc.R.Soc.A, 463, 837-854 [https://doi.org/10.1098/rspa.2006.1798].

Townend, I.H., Wang, Z.B., Stive, M.J.E., Zhou, Z., 2016a. Development and extension of an aggregated scale model: Part 1 – Background to ASMITA. China Ocean Engineering, 30(4), 482-504 [https://doi.org/10.1007/s13344-016-0030-x].

Townend, I.H., Wang, Z.B., Stive, M.J.E., Zhou, Z., 2016b. Development and extension of an aggregated scale model: Part 2 – Extensions to ASMITA. China Ocean Engineering, 30(5), 651-670 [https://doi.org/10.1007/s13344-016-0042-6].

van der Spek, A.J.F., Beets, D.J., 1992. Mid-Holocene evolution of a tidal basin in the western Netherlands: a model for future changes in the northern Netherlands under conditions of accelerated sea-level rise? Sedimentary Geology, 80, 185-197 [https://doi.org/10.1016/0037-0738(92)90040-x].

van der Wegen, M., Wang, Z.B., Townend, I.H., Savenije, H.H.G., Roelvink, J.A., 2009. Long-term, morphodynamic modeling of equilibrium in an alluvial tidal basin using a process-based approach. River, Coastal and Estuarine Morphodynamics.

van Goor, M.A., Zitman, T.J., Wang, Z.B., Stive, M.J.F., 2003. Impact of sea-level rise on the morphological equilibrium state of tidal inlets. Marine Geology, 202, 211-227 [https://doi.org/10.1016/s0025-3227(03)00262-7].

van Rijn, L.C., 1993. Principles of sediment transport in rivers, estuaires and coastal seas. Aqua Publications, Amsterdam.

Vermeersen, L.L.A., Slangen, A.B.A., Gerkema, T., Baart, F., Cohen, K.M., Dangendorf, S., Duran-Matute, M., Frederikse, T., Grinsted, A., Hijma, M.P., Jevrejeva, S., Kiden, P., Kleinherenbrink, M., Meijles, E.W., Palmer, M.D., Rietbroek, R., Riva, R.E.M., Schulz, E., Slobbe, D.C., Simpson, M.J.R., Sterlini, P., Stocchi, P., van de Wal, R.S.W., van der Wegen, M., 2018. Sea level change in the Dutch Wadden Sea. Netherlands Journal of Geosciences, 97(3), 79-127 [https://doi.org/10.1017/njg.2018.7].

Wang, Z.B., 1992. Theoretical analysis on depth-integrated modelling of suspended sediment transport. Journal of Hydraulic Research, 30(3), 403-420 [https://doi.org/10.1080/00221689209498927].

Wang, Z.B., de Vriend, H.J., Stive, M.J.F., Townend, I.H., 2008. On the parameter setting of semi-empirical long-term

morphological models for estuaries and tidal lagoons. In: C.M. Dohmen-Janssen, S.J.M.H. Hulscher (Eds.). River, Coastal and Estuarine Morphodynamics. Taylor & Francis, pp. 103-111 [https://doi.org/10.1201/noe0415453639-c14].

Wang, Z.B., Elias, E.P.L., van der Spek, A.J.F., Lodder, Q.L., 2018. Sediment budget and morphological development of the Dutch Wadden Sea - impact of accelerated sea-level rise and subsidence until 2100. Netherlands Journal of Geosciences, 97(3), 183-214 [https://doi.org/10.1017/njg.2018.8].

Wang, Z.B., Hoekstra, P., Burchard, H., Ridderinkhof, H., de Swart, H.E., Stive, M.J.F., 2012. Morphodynamics of the Wadden Sea and its barrier island system. Ocean & Coastal Management, 68(0), 39-57 [https://doi.org/10.1016/j.ocecoaman.2011.12.022].

Wang, Z.B., Karssen, B., Fokkink, R.J., Langerak, A., 1998. A dynamic-empirical model for estuarine morphology. In: J. Dronkers, M.B.A.M. Scheffers (Eds.), Physics of Estuaries and Coastal Seas. Balkema, Rotterdam, pp. 279-286.

Wang, Z.B., Townend, I.H., 2012. Influence of the nodal tide on the morphological response of estuaries. Marine Geology, 291-294, 73-82 [https://doi.org/10.1016/j.margeo.2011.11.007].

Winterwerp, J.C., van Kesteren, W.G.M., van Prooijen, B., Jacobs, W., 2012. A conceptual framework for shear flow–induced erosion of soft cohesive sediment beds. Journal of Geophysical Research, 117(C10), [https://doi.org/10.1029/2012jc008072].

Wright, A.D., Townend, I.H., 2006. Predicting long term estuary evolution using regime theory. Littoral 2006 Conference Proceedings. Gdansk University of Technology, Faculty of Management and Economics, Traugutta 79, pp. 1-9.

Supplementary Information for

Aggregated morphodynamic modelling of tidal inlets and estuaries

Zheng Bing Wang[1,2,4], Ian Townend[1,3], Marcel Stive[1,2]

1 College of Harbor, Coastal and Offshore Engineering, Hohai University, Nanjing, China
2 Department of Hydraulic Engineering, Faculty of Civil Engineering and Geosciences, Delft University of Technology, Delft 2600GA, the Netherlands
3 School of Ocean and Earth Sciences, University of Southampton, Southampton, UK
4 Deltares, Delft, the Netherlands

The basis of the hydrodynamics, morphological equilibrium state, sediment transport and morphological changes used in ASMITA are detailed below. This is presented in terms of 3 geomorphological elements, namely Delta, Channel and Tidal flat. For details of the formulation of an ASMITA model using multiple elements see Kragtwijk et al. (2004) and Townend et al (2016).

SI.1 - Hydrodynamics

If the morphology of a tidal inlet system is only defined by the volumes of the three morphological elements mentioned above (see also Fig.1) it does not need to model the hydrodynamics in detail. In fact, only the tidal range in the back-barrier basin and the tidal prism are needed to define the morphological equilibrium state. Tidal basins, such as those in the Wadden Sea, are relatively small with respect to the tidal wavelength. For such short basins it is acceptable to use the water volume between high and low water for the tidal prism. When the intertidal volume is defined in terms of sediment volume, the relation between the tidal range H and the tidal prism P is given by:

$$P = A_b H - V_f \tag{S.1}$$

Herein A_b is the horizontal area of the basin at MHW. The tidal range in the basin is dependent on the tidal range in the open sea as well as dependent on the morphological state of the tidal inlet system. The tidal range in the open sea should be considered as a boundary condition. It is difficult to model the influence of the morphological changes on the tidal range due to the highly aggregated schematisation. However, for short basins like those in the Wadden Sea, the influence of the morphological changes on the tidal range is limited. Therefore, the tidal range in the basin H is prescribed. It is noted that it is still possible to have H varying in time, to take account of any trend or a cyclic change e.g. the nodal tide variation (Jeuken et al., 2003; Wang and Townend, 2012). It is also noted that the model does consider the feedback from the morphological development to the hydrodynamics, via Eq. (10), because V_f is a morphological state variable.

SI.2 - Morphological equilibrium state

For all three elements, empirical relationships are required to define their morphological equilibrium dimensions. With these relationships the morphological equilibrium state of a tidal basin is fully determined if the basin area A_b and the tidal range H are given. The equilibrium relationships can be prescribed in various ways (see Townend et al, 2016). Here we outline the approach that has been used to study the dynamics of the Wadden Sea.

For the intertidal flat there are two empirical relationships used, one for its area and one for its height (Renger and Partenscky, 1974, Eysink and Biegel, 1992).

$$\frac{A_{fe}}{A_b} = 1 - 2.5 \cdot 10^{-5} \sqrt{A_b} \tag{S.2}$$

$$h_{fe} = \alpha_{fe} H \tag{S.3}$$

Herein A_{fe} [m^2] is the equilibrium tidal flat surface area; A_b [m^2] is basin surface area; H is tidal range

and according to Eysink (1990)

$$\alpha_{fe} = \alpha_f - 0.24 \cdot 10^{-9} A_b \tag{S.4}$$

with α_f = 0.41. The equilibrium volume of the intertidal flat, i.e. the sediment volume between low water (MLW) and high water (MHW), is thus by definition:

$$V_{fe} = A_{fe} h_{fe} \tag{S.5}$$

The channel volume V_c is defined as the water volume under MLW in the basin. Its equilibrium value is related to the tidal prism as follows:

$$V_{ce} = \alpha_c P^{1.55} \tag{S.6}$$

The equilibrium volume of the ebb tidal delta is also related to the tidal prism (Walton and Adams, 1976)

$$V_{de} = \alpha_d P^{1.23} \tag{S.7}$$

Using these equations with various empirical coefficients (the α's) the morphological equilibrium of a tidal basin can be determined from two parameters, the total basin area A_b and the tidal range H. For a single element model for the back-barrier basin the total water volume of the basin below MHW, which is the sum of the channel volume (below LW) V_c and the tidal prism P, can be used:

$$V = V_c + P \quad \text{and} \quad V_e = F\left(A_b, H\right) \tag{S.8}$$

SI.3 - Sediment transport and morphological change

As explained in the previous section, the sediment transport processes are described by the mass-balance equation for sediment for each of the element aggregated in time (Eq. 7). Following the schematisation shown in Fig.1 these equations are:

$$J_{cf} + F_{Bf} = 0 \tag{S.9}$$

$$J_{dc} - J_{cf} + F_{Bc} = 0 \tag{S.10}$$

$$J_{od} - J_{dc} + F_{Bd} = 0 \tag{S.11}$$

In these equations J is the sediment transport, and its subscripts indicate from which element to which element (f = flat, c = channel, d = ebb tidal delta, o = outside world). J_{cf} is thus the sediment transport from the element channel to the element flat. F_B is sediment exchange flux between the bed and the water column. Because of the aggregation in time, the transports are governed by the diffusion / dispersion with the tidal flow as mixing agent:

$$J_{cf} = \delta_{cf}\left(c_c - c_f\right) \tag{S.12}$$

$$J_{dc} = \delta_{dc}\left(c_d - c_c\right) \tag{S.13}$$

$$J_{od} = \delta_{od}\left(c_o - c_d\right) \tag{S.14}$$

In these equations c is suspended sediment concentration, and its subscript indicates the morphological element. δ is the horizontal exchange coefficient with the dimension [L^3T^{-1}] and depends on the dispersion coefficient, the area of the cross-section connecting the two elements and the distance between the two elements (see Wang et al., 2008). Its subscripts have similar meaning as those of J.

F_B is the sediment exchange flux between bed and water representing erosion minus sedimentation. Its second subscript again indicates the morphological element. Like Eq.(7) they are formulated as follows:

$$F_{Bf} = w_f A_f \left(c_{fe} - c_f\right) \tag{S.15}$$

$$F_{Bc} = w_c A_c \left(c_{ce} - c_c\right) \tag{S.16}$$

$$F_{Bd} = w_d A_d \left(c_{de} - c_d \right) \tag{S.17}$$

In these equations A is the horizontal area of the element and w is the vertical exchange velocity, which is proportional to the settling velocity of sediment (see Eq.7). Their subscripts indicate the element. Note that the vertical exchange velocity is not necessarily the same for all three elements even if only a single fraction of sediment is present. As discussed earlier, the equilibrium sediment concentrations are calculated by comparing the morphological state with its equilibrium for each of the elements:

$$c_{fe} = C_f \left(\frac{V_f}{V_{fe}} \right)^{n_f} \tag{S.18}$$

$$c_{ce} = C_c \left(\frac{V_{ce}}{V_c} \right)^{n_c} \tag{S.19}$$

$$c_{de} = C_d \left(\frac{V_d}{V_{de}} \right)^{n_d} \tag{S.20}$$

In these equations, the coefficients C have the dimension of sediment concentration and n is a power similar to that in a power-law sediment transport formula (Wang et al., 2008). Note the difference in the formulations between the elements flat and delta with a sediment volume as morphological state variable and the channel element with water volume as state variable (sediment volume relationships are the inverse of the water volume relationship).

The sediment exchange between bed and water (Eqs.S.15-S.17) also determines the change of the morphological state variable of the corresponding element:

$$\frac{\mathrm{d}V_f}{\mathrm{d}t} = -F_{Bf} = -w_f A_f \left(c_{fe} - c_f \right) \tag{S.21}$$

$$\frac{\mathrm{d}V_c}{\mathrm{d}t} = F_{Bc} = w_c A_c \left(c_{ce} - c_c \right) \tag{S.22}$$

$$\frac{\mathrm{d}V_d}{\mathrm{d}t} = -F_{Bd} = -w_d A_d \left(c_{de} - c_d \right) \tag{S.23}$$

If all morphological elements in the whole system are in equilibrium, F_B should vanish for all elements, thus the sediment concentration is equal to its equilibrium value for each of the elements ($c_f=c_{fe}$, $c_c=c_{ce}$, $c_d=c_{de}$). The equations (S.9)-(S.11) yield: $J_{cf}=J_{dc}=J_{od}=0$, i.e. all residual sediment transports vanish, and it follows then from equations (S.12)-(S.14) that $c_f=c_c=c_d=c_o$, and thus also $c_{fe}=c_{ce}=c_{de}$. According to equations (S.18)-(S.20) $c_{fe}=C_f$, $c_{ce}=C_c$, $c_{de}=C_d$ if all the elements are in equilibrium (their volumes equal to their equilibrium values). Now it follows $C_f=C_c=C_d=c_o$. Thus, the coefficients in equations (S.18)-(S.20) should be the same and equal to the sediment concentration at the open boundary (the outside world). This constant is called the global equilibrium concentration C_E:

$$C_f = C_c = C_d = c_o = C_E \tag{S.24}$$

Any deviation from this rule implies a redefinition of the morphological equilibrium state.